Model Predictive Control (MPC) and Proportional Integral Derivative Control (PID) for Autonomous Lane Keeping Maneuvers: A Comparative Study of Their Efficacy and Stability

Ahsan Kabir Nuhel[1](✉), Muhammad Al Amin[1], Dipta Paul[1], Diva Bhatia[2], Rubel Paul[3], and Mir Mohibullah Sazid[1]

[1] American International University, Kuratoli, Bangladesh
nuhel7050@gmail.com
[2] Vellore Institute of Technology, Vellore, India
[3] Sonargaon University, Dhaka, Bangladesh

Abstract. The escalating frequency of fatal crashes has led to an enhanced focus on road safety, resulting in the creation of diverse driver assistance systems. Several instances of these systems encompass active braking, lane departure warning, cruise control, lane maintaining, and numerous additional examples. However, the primary objective of this research is to examine the effectiveness and reliability of a model predictive control (MPC) and a proportional integral derivative (PID) control in executing lane keeping maneuvers within an autonomous vehicle. In this paper, a custom controller for autonomous lane-changing maneuvers is developed by utilizing the Model Predictive Control (MPC) and Proportional-Integral-Derivative (PID) controllers. Different trajectory models are employed to assess the overall effectiveness of the designed model, showcasing its superiority over existing models.

Keywords: Autonomous car · Trajectory models · MPC · PID · Model Prediction

1 Introduction

Autonomous vehicle is one of key technological advancement to keep the road safe and decrease the number of fatal accidents [1]. Apart from than, most of the modern cars come with Advance Driving Assistance System (ADAS) to help the driver in the road. The main functions for these kinds of systems are autonomous breaking, lane keeping assist, object detection, lane departure warning and so on. In this project, a custom controller have designed to keep the car in the lane [2]. At first, Kinematic Bicycle model is discussed which is used to design the MPC controller.

P. Pareek et al. (Eds.): IC4S 2023, LNICST 537, pp. 107–121, 2024.
https://doi.org/10.1007/978-3-031-48891-7_9

While designing the MPC controller, as inputs, this method considers the current condition of the vehicle, including its position, velocity, and heading, as well as the positions of surrounding vehicles [3]. System dynamic is also taken into consideration to fulfill the control objective. Different trajectory models are generated to observe the models and checking the outputs with the pre-existing models [4]. The results are analyzed with reference trajectory, straight and curve trajectory for different attributes.

The paper is divided into five sections. In Sect. 2, the paper describes earlier fundamental research concepts. Section 3 describes the proposed methodology and experimental setup. Section 4 analyzes the results, and Sect. 5 discusses potential future applications.

2 Literature Review

In the research of Trajectory Tracking Control using MPC Controller for of Quadcopter [5], G. Ganga and co-author Meher Madhu Dharmana constructed a quadcopter by utilising the dynamic equation in 2017. They proceeded to devise a linear Model Predictive controller and a Proportional-Integral-Derivative controller to address the issue of trajectory tracking for the quadcopter. The findings of this study demonstrate the superiority of the Linear Model Predictive controller over the Proportional-Integral-Derivative controller in the context of design objectives.

In a paper Hengyang Wang, Biao Liu, Xianyao Ping, and Quan worked on Autonomous Vehicles Path Tracking Control Based on an Improved Model Predictive Controller. They proposed an enhanced MPC controller that incorporates fuzzy adaptive weight control. The objective of their study is to address the challenge of lane tracking in autonomous vehicles. The fuzzy adaptive control algorithm is employed to implement this controller, which primarily involves the cost function by dynamically increasing the weight in the classical model predictive control (MPC) approach.

In 2020 Shuping Chen, Huiyan Chen, and Dan Negrut worked on the study of Path Tracking for Autonomous Vehicles with the Implementation of Model Predictive Control Incorporating Three Vehicle Dynamics Models with Varying Fidelities. They proposed the practical application of path tracking for autonomous vehicles. In the study conducted by [7], an MPC controller was developed utilising three distinct models: an 8-DOF model, the bicycle model, and a 14-DOF model. The reference paths employed in the experiment consisted of a straight line and a circular trajectory. The researchers also conducted a comparative analysis of the performances exhibited by various models.

Ak Nuhel, MM Sazid and MNM Bhuiyan designed a level 5 autonomous car using machine learning, deep learning and CNN [8]. Apart from that, MPC controller is used to design the path of the car using different trajectory analysis. An overview of vehicle safety was also discussed.

In the paper, Eugenio Alcalá, Vicenç Puig, and Joseba Quevedo worked on "LPV-MPC Control for Autonomous Vehicles" [9] in 2019. They addressed a trajectory tracking issue pertaining to autonomous vehicles. The approach employs a cascade control strategy, wherein an external loop is utilised for position control through the implementation of a Learning Parameter Varying (LPV) Model Predictive Control (MPC) controller. The distinction between the LPV-MPC controller and the Nonlinear (NL) MPC

controller is demonstrated, and the superior performance of the LPV-MPC controller is discussed.

3 Methodology

3.1 Vehicle Model

According to Limebeer and Massaro [10], the vehicle model serves as a fundamental basis for investigating the features of vehicle control. Consequently, an accurate vehicle model is crucial for developing a reliable and precise model of vehicle control. Both the kinematic bicycle model and the dynamic bicycle model are analyzed in detail in this research, for the purpose of implementing autonomous driving capabilities in our vehicle. The utilization of models is imperative for conducting an in-depth analysis of vehicles, particularly for the purpose of modeling the controller.

Kinematic Bicycle Model.
The motion of a bicycle can be conceptualized within the theoretical framework of the Kinematic Bicycle Model.

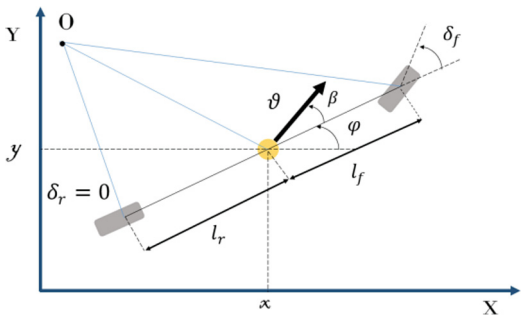

Fig. 1. Kinematic Bicycle model

The studies by Rajamani and Zhang [2] show that the kinematic bicycle model is commonly used in the study of vehicle features [11]. Figure 1 demonstrates the kinematic bicycle model. There are four wheels total, two in the front and two in the back, however in this model they function as one. The forward lumped wheel sits precisely in the geometric center of the front axle, whereas the rear lumped wheel is centered on the back axle. The kinematic model can be quantitatively expressed by Eqs. (1) through (5) if it is assumed that the front wheel is the only part responsible for steering.

$$\dot{x}\, vcos(\psi + \beta), \tag{1}$$

$$\dot{y}\, vsin(\psi + \beta), \tag{2}$$

$$\dot{\psi}\, \frac{v}{l_r}(\beta), \tag{3}$$

$$\dot{v}\, a \tag{4}$$

$$\beta \arctan\left(\frac{l_r}{l_f + l_r} + \tan(\delta_f)\right)\Bigg) \tag{5}$$

The inertial frame's center of mass is represented by the coordinates (X,Y), where X and Y are variables. The direction of the self-driving car's movement is indicated by ψ and its velocity is marked by the variable v. Distances from the center of mass to the front and rear wheels are represented by the l_f and l_r variables, respectively. The present model incorporates acceleration (a) and the stecring angle (δ) as control inputs. In order to simplify the analysis and facilitate practical application, it is common practice to assume that the rear wheels of a vehicle have zero steering angle $\delta_r = 0$, with the focus being solely on the steering of the front wheel. The present kinematic model exhibits a relatively elementary structure in comparison to alternative models that incorporate additional physical factors such as aerodynamic drag, gravitational force, and frictional resistance. The kinematic model can be identified with only two parameters, namely (l_f and l_r), rendering it applicable for both longitudinal and lateral control purposes.

3.2 Controller Design

The controller utilizes Model Predictive Control (MPC) as its fundamental approach. This method takes into account the present states of the vehicle, including its position, velocity, and heading, as well as the positions of neighboring vehicles, as inputs [12]. The output of the MPC is a set of acceleration and steering angle values (Fig. 2).

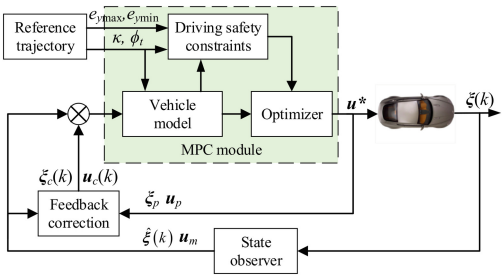

Fig. 2. Stabilization via Model-Predictive Controlling High-Speed Autonomous Ground Vehicle

System Dynamics.
The study utilizes a nonlinear kinematic bicycle model to depict the characteristics of vehicle dynamics [3]. The kinematics are rewritten here for completeness from Eq. 6 to 10:

$$\dot{x} = vcos(\psi + \beta) \tag{6}$$

$$\dot{y} = vsin(\psi + \beta) \tag{7}$$

$$\dot{\psi} = \frac{v}{l_r} sin(\beta) \tag{8}$$

$$\dot{v} = a \tag{9}$$

$$\beta = tan^{-1}\left(\frac{l_r}{l_f + l_r} tan(\delta)\right) \tag{10}$$

Cartesian coordinates (x, y) represent the location of the vehicle's center of mass, whereas the inertial heading ψ is the direction in which the vehicle is moving. The variable v stands for the speed of the car, while the letter a stands for the acceleration felt by the vehicle's center of mass in the direction of the speed. Distances from the vehicle's center to the front and rear axles are denoted by the l_f and l_r variables. Both the front wheel's steering angle (δ) and the vehicle's acceleration (a) are used as inputs for control. The following mathematical representation captures the essence of the discrete-time dynamical model derived by the Euler discretization method:

$$z(t+1) = f(z(t), u(t)) \tag{11}$$

where $z = \begin{bmatrix} x\ y\ \psi\ v \end{bmatrix}^\top$ and $u = \begin{bmatrix} a\ \delta \end{bmatrix}^\top$ (12) for time t.

Control Objective.

The principal goal of the control system is to effectively integrate into the designated lane, while concurrently avoiding any potential collisions with other vehicles. We have a predilection for changing lanes at a prior intersection. Enhanced driving comfort is typically associated with a preference for smooth accelerations and steering. The presentation of the objective function formulation is as follows:

$$J = \sum_{\ell=t}^{t+T} \lambda_{div}(x(\ell \mid t); x_{end}) D(\ell \mid t) \tag{12}$$

$$+ \sum_{\ell=t}^{t+T} \lambda_v \| v(\ell \mid t) - v^{ref} \|^2 \tag{13}$$

$$+ \sum_{\ell=t}^{t+T-1} \lambda_\delta \parallel \delta(\ell \mid t) \parallel^2 \tag{14}$$

$$+ \sum_{\ell=t}^{t+T-1} \lambda_a \parallel a(\ell \mid t) \parallel^2 \tag{15}$$

$$+ \sum_{\ell=t+1}^{t+T-1} \lambda_{\Delta\delta} \parallel \delta(\ell \mid t) - \delta(\ell - 1 \mid t) \parallel^2 \tag{16}$$

$$+\sum_{\ell-t+1}^{t+T-1} \lambda_{\Delta a} \parallel a(\ell \mid t) - a(\ell - 1 \mid t) \parallel^2 \tag{17}$$

The temporal value of l is determined by the data collected at time t, and is denoted by the symbol $(l|t)$. The latitude coordinate of the road's terminus is represented by the symbol x_{end}. The ego vehicle's distance norm to the target lane at time l is denoted by $D(l|t)$. The symbol v^{ref} refers to the reference velocity. The regularization of each penalty is accomplished by employing λ_{div}, λ_v, λ_δ, λ_a, $\lambda_{\Delta\delta}$, and $\lambda_{\Delta a}$,, correspondingly. The timely lane change is incentivized through the utilization of a dynamic weight, denoted as λ_{div},, which is expressed as a convex function. Specifically, λ_{div} is represented as $\| \frac{1}{x_{\text{end}} - x} \|$. The aforementioned expression denoted by (12) serves to penalize the deviation of the car's center from the vertical midpoint of the designated lane. The expressions denoted by (14) and (15) serve to impose a penalty on the exertion of control in relation to the steering angle and acceleration, respectively. To improve ride quality, the steering rate and disturbance is impacted by the equations labelled as (12) and (12), respectively.

Transitional Model Predictive based Controlling for Lane Changing.
To avoid rear-end crashes during overtaking maneuvers, autonomous trajectory path tracking using Model Predictive Control is implemented [14]. In Fig. 4 we see a model of the control architecture used by the autonomous vehicle. For making a lane change, the major focus for designing trajectories is to reduce the amount of yaw acceleration the vehicle experiences. The constraints pertaining to the dynamics of vehicles and the boundaries of the roadside are articulated as limitations within a set of convex optimization problems. The acquisition of reference positions and velocities is achieved through the utilization of a convex optimization algorithm. Model Predictive Control (MPC) controllers, like the one seen in Fig. 4, make use of mathematical models of autonomous cars to anticipate how the system would evolve in the future. This methodology is employed to enhance future vehicle performance and minimize the discrepancy between the planned trajectory route and the actual route (Fig. 3).

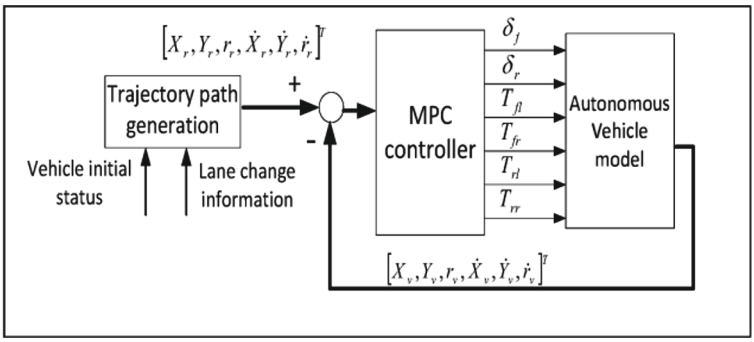

Fig. 3. Architecture for the management of systems in autonomous vehicles.

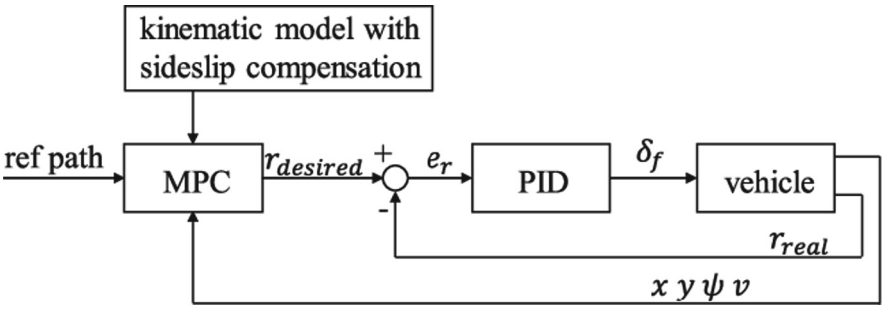

Fig. 4. The Lateral Control configuration of the proposed model

PID Controller

The study presents a PID controller that is specifically designed to ensure that the vehicle adheres to a desired yaw rate [13], $\dot{\psi}$, while simultaneously minimizing the sideslip, β. Equation (18) pertains to the pid control law. This consists of K_p, K_i, and K_d, the proportional, integral, and derivative gains, respectively. These three parts work together to form the G_c block of the controller transfer function.

$$G_c = K_p + \frac{K_i}{s} + K_d s \tag{18}$$

K_p, K_i and K_d values were obtained using the built-in tuning tool in MATLAB SIMULINK and was imported in coding script., as presented in Table 1. In order to evaluate the efficacy and purpose of control techniques during vehicular maneuvers, distinct control parameters are established for each test velocity to enhance the system's response.

Table 1. PID Tuning Parameters

Control Parameters	Speed	
	Slow 30 km/h	High 80 km/h
K_d	3	0.03
K_p	7	0.81
K_i	5	8.10

3.3 Development of Trajectory Generator and Tracking Controller

The development of a trajectory tracking controller is a crucial area of research in the field of control systems. This controller aims to enable precise tracking of desired trajectories by a dynamic system. By utilizing advanced control algorithms and sensor feedback, the trajectory tracking controller enhances the system's ability to follow predefined paths

accurately, facilitating applications in various domains such as robotics, autonomous vehicles, and aerospace. Prediction Model Development employs a nonlinear dynamic system that takes into account the output:

$$\dot{\xi}(t) = f(\xi(t), \mu(t)) \tag{19}$$

$$\eta(t) = h(\xi(t), \mu(t)) \tag{20}$$

The following expression includes the state transition function f(.,.), a state variable $\xi(t)$ with n dimensions, a control variable $\mu(t)$ with m dimensions, and an output variable $\eta(t)$ with p dimensions.

Convert the continuous systems of Eqs. (17) and (18) into a linear time-varying system.

$$\xi(k+1) = A_{k,t}\xi(k) + B_{k,t}\mu(t) + d_{k,t} \tag{21}$$

$$\eta(t) = C_{k,t}\xi(k) + D_{k,t}\mu(t) + e_{k,t} \tag{22}$$

Taking into account the following presumptions:

$$\acute{A}_{k,t} = \begin{bmatrix} A_{k,t} & B_{k,t} \\ 0_{m\times n} & I_m \end{bmatrix} \tag{23}$$

$$\acute{B}_{k,t} = \begin{bmatrix} B_{k,t} \\ I_m \end{bmatrix} \tag{24}$$

$$\acute{C}_{k,t} = [C_{k,t} \quad D_{k,t}] \tag{25}$$

$$\acute{D}_{k,t} = D_{k,t} \tag{26}$$

$$\acute{\xi}(k|t) = \begin{bmatrix} \xi(k|t) \\ \mu(k-1|t) \end{bmatrix} \tag{27}$$

$$\acute{d}(k|t) = \begin{bmatrix} d(k|t) \\ 0_m \end{bmatrix} \tag{28}$$

The symbol $0_{m\times n}$ represents a zero matrix with dimensions $m \times n$, while I_m denotes an identity matrix with dimensions m.

When designing the trajectory tracking controller, it is imperative to take into account the constraints imposed by the vehicle dynamics.

3.4 The Constraint of Sideslip Angle at the Mass Center

Significant changes in driving stability can occur when the mass center's sideslip angle β is outside the linear range of the lateral force, necessitating the imposition of constraints.

The mass center slip angle's constraint range is commonly represented by the arctangent function.

$$-arctan(0.02\mu g) \leq \beta \leq arctan(0.02\mu g) \tag{29}$$

The Constraint of Lateral Acceleration

The amount of grip provided by a car's tires on the road has a direct impact on the vehicle's performance. The presence of different coefficients of adhesion on the road results in the generation of distinct longitudinal and lateral forces that are applied to the Tire by the ground. This research establishes a connection between forward velocity, sideways velocity, and road adhesiveness, highlighting the presence of inequality in this relationship. The inequality of the given expression is as follows.

$$\sqrt{a_x^2 + a_y^2} \leq \mu g \tag{30}$$

can be presented, where the acceleration along the longitudinal axis is denoted by a_x and the acceleration perpendicular to it is denoted by a_y. The longitudinal velocity of the vehicle showed almost no variation during a relatively short time period. It is reasonable to hypothesize that the vehicle maintains a constant longitudinal speed. As a result, Eq. (30) can be simplified in the subsequent manner.

$$\left|a_y\right| \leq \mu g \tag{31}$$

The inability to accurately calculate can be ascribed to the constraint conditions being either overly inclusive or overly restrictive, depending on the specific road adhesion circumstances. A relaxation coefficient is included in to provide the adaptive modification of constraint conditions in response to the solution scenario of each control iteration, making the restriction on lateral acceleration a flexible constraint. This inequality holds for every value of the lateral acceleration $\left|a_y\right| \leq \mu g$:

$$a_{y,min} - \varepsilon \leq a_y \leq a_{y,max} + \varepsilon. \tag{32}$$

The maximum and minimum lateral accelerations, $a_{y,max}$ and $a_{y,min}$, are shown below, where ε stands for the relaxation factor.

3.5 Experimental Setup

The experiment was set up in simulation using the command prompt of Windows version 11 to execute the main file and a support file for backing up library functions. Python version 3.7, along with NumPy and Matplotlib libraries, was utilized for the process, while separate animation scripts were incorporated for visualizations. The experiment involved constants related to an autonomous vehicle and model parameters, which are detailed in Table 2, allowing researchers and engineers to analyze their impact on the vehicle's behavior and the model's performance.

Table 2. Dimensions of the car model and other environmental attributes

Parameters	Values
Mass (m)	1500 g
Mass moment of inertia (I_z)	3000 g
Front wheel cornering stiffness (C_{af})	19000 N/m
Back wheel cornering stiffness (C_{ar})	33000 N/m
The gap between the front wheel and the mass (L_f)	2 c.m
The gap between the back wheel and the mass (L_r)	3 c.m
Sampling time (T_s)	0.02 s
Lane width	7 m
Number of lanes	5
Reference Trajectory frequency	0.01 Hz

4 Results Analysis

The author of the study devised three distinct trajectory models to assess the efficacy and performance of the overall system under investigation (Fig. 5). These systems were meticulously engineered and implemented to evaluate different aspects and functionalities of the overarching system. The accompanying visual aids, presented below, depict specific instances where a car adeptly tracks and follows its designated reference trajectory. In these illustrations, the reference trajectory is represented by the blue color, while the actual position of the vehicle is denoted by the red color. These visual representations vividly showcase the successful execution of the implemented control algorithms and highlight the capability of the system to accurately adhere to the desired trajectory while maintaining the desired position).

The front wheel demonstrated smooth movement and effectively adjusted its position to accommodate both positive and negative slopes as required by the system, effectively avoiding overshooting. When analyzing the hybrid parabola scenario, a minor delay was observed during the initial response, and the front wheel exhibited aggressive behavior. This behavior can be attributed to the fact that, initially, the vehicle was oriented in the x-direction with a yaw angle of 0 radians, while the reference yaw angle was set to 0.5 radians at time 0 s. Consequently, there was a noticeable deviation in tracking the predetermined setpoint. As the vehicle gradually aligned itself with the desired setpoint, its velocity decreased, leading to a more consistent speed. Additionally, it was noted that the steering wheel angle reached its maximum limit of *pi/6* radians during this specific instance (showcases in Fig. 6).

From the analysis presented in Fig. 7, it becomes evident that the controller's performance deteriorates when operating at higher frequencies. This degradation can be attributed to the fact that the car's longitudinal velocity remains unchanged, leaving insufficient time for the system to stabilize, despite the amplitude of the input signal not being significantly marginal. To overcome this limitation, the longitudinal velocity was

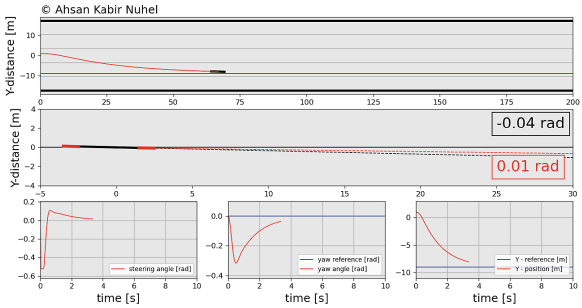

(a) Car following reference trajectory in a straight line

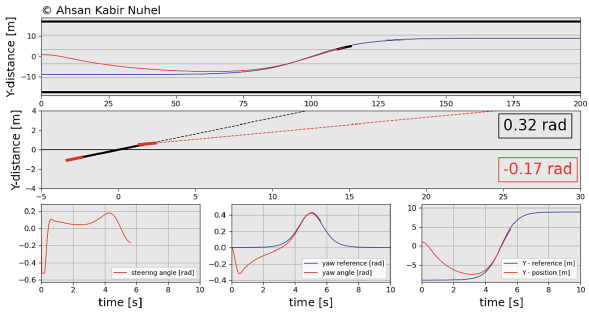

(b) Car following reference trajectory in a curvy line

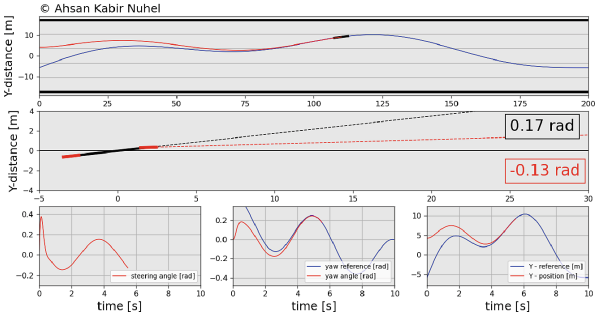

(c) Car following reference trajectory in a hybrid (Mixed trajectory of sinusoidal and parabolic) line

Fig. 5. Car's attributes in following difference reference trajectories

subsequently adjusted to a value of 20 m/s. Particularly, the experiments show that the vehicle can successfully follow a reference input's optimally trajectory. Moving on to Fig. 8, we observe the output pertaining to variations in higher weight matrices within the cost function for both state and final horizon period outputs. The outcomes reveal a proportional relationship between the weight values and the minimization of specific

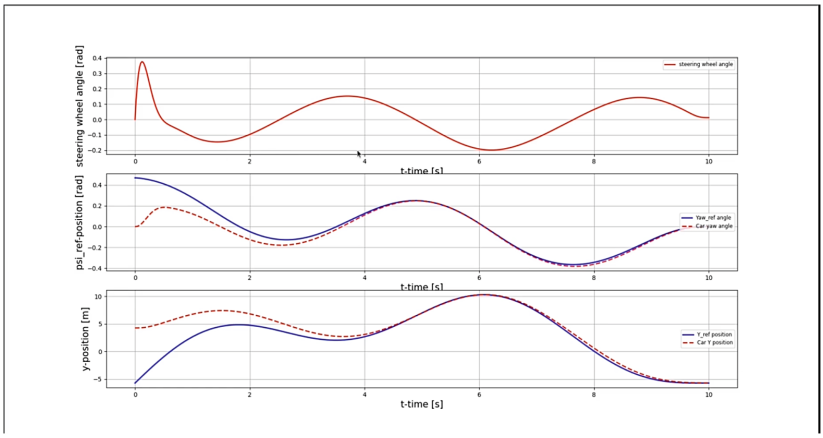

Fig. 6. Different attributes of car at following curvy line trajectory

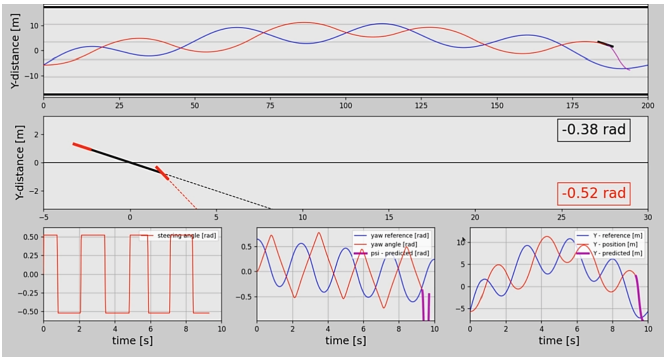

Fig. 7. Model attributes at frequency 0.01 Hz

errors associated with either the yaw reference angles or the vehicle's position. Consequently, the error in the yaw angle significantly diminishes in comparison to the larger positional error, thereby validating the efficacy of the approach.

According to the findings presented in Fig. 9, the incorporation of the Proportional-Integral-Derivative (PID) controller resulted in observable oscillation in both the steering wheel and yaw reference angle. This phenomenon arises due to the fact that the PID controller solely considers errors within a single sampling time and lacks the ability to take into account the entire time horizon, unlike the Model Predictive Control (MPC) controller. Therefore, the task of fully mitigating overshooting becomes a challenging attempt for the PID controller. On the other hand, due to the MPC controller's ability to make more informed decisions by utilising future predictions derived from the system model, the oscillations and error reduction achieved are significantly smoother in comparison to those obtained with the PID controller.

Furthermore, to assess the overall effectiveness of the proposed model, three distinct trajectories were formulated. Among these trajectories, only the exponential and

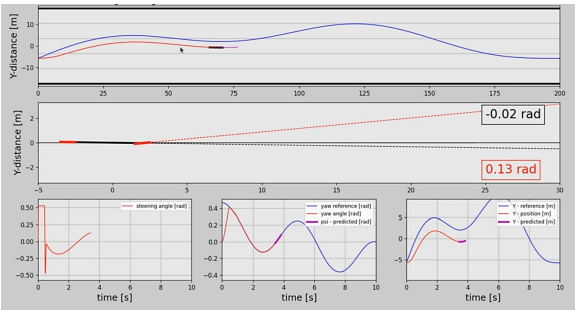

Fig. 8. Outputs concerning changing in the weight matrices by breaking the identity law (by prioritizing Yaw angle error)

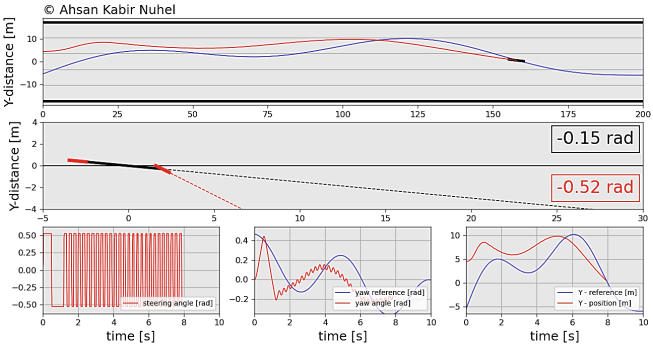

Fig. 9. Output concerning PID controller.

cubic polynomials were considered, and their corresponding outcomes are depicted in Figs. 10 and 11. The results exhibit a satisfactory tracking performance characterized by consistent and accurate adherence to the prescribed reference setpoints, while maintaining a desirable level of smoothness. It is worth noting that the vehicle's initial course angle is set to zero, whereas the initial course angle of the reference trajectory exceeds zero. Consequently, the vehicle demonstrates the ability to adjust its direction during this phase. This modification enables accurate monitoring of the reference trajectory, thereby improving both the resilience and precision. As the vehicle's speed increases and the adhesion coefficient of the road surface reduces, the aforementioned simulation findings show that noticeable deviations from the desired trajectory are noticed when using double-shifting. Moreover, such deviations may give rise to hazardous situations where the vehicle loses control over its direction.

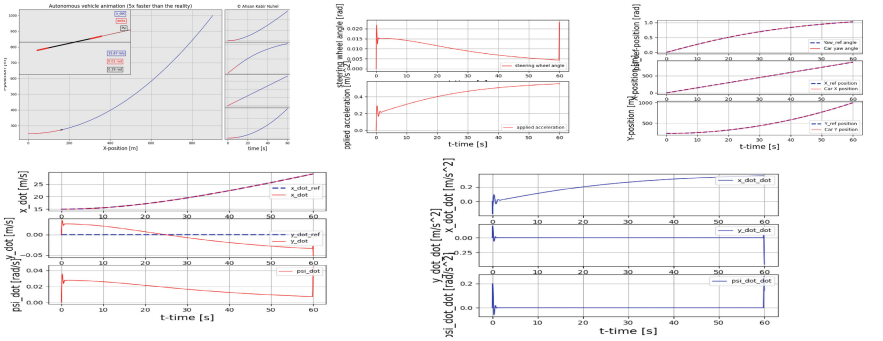

Fig. 10. Results pertaining exponential route

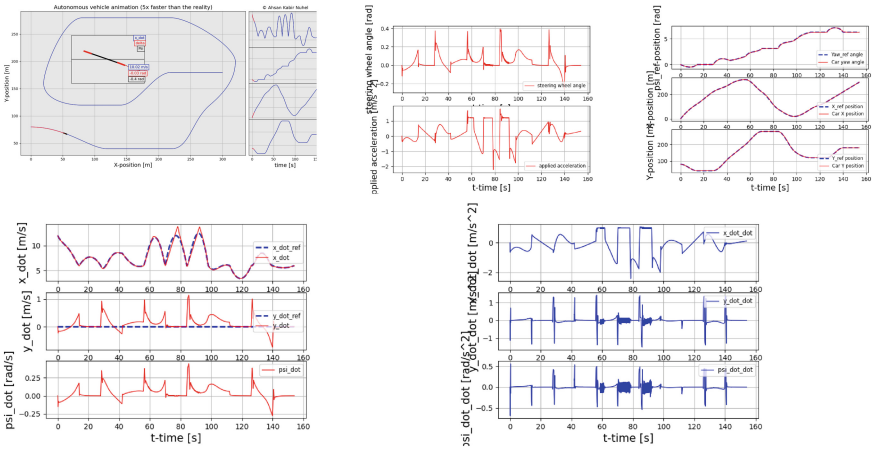

Fig. 11. Results pertaining cubic polynomial route

5 Conclusion

The paper uses a MPC controller to track the path of any cars. It can be used in ADAS or Autonomous cars for keeping the vehicle in lane. For the modern safety requirements, it important have ADAS in every modern vehicle [14]. This MPC controller can meet one of the key features in ADAS system. The paper analysis the different trajectory of the car using the custom made MPC controller and shows how it is better than pre-existing controller such as PID controller. The vehicle movement and speed also taken into consideration while doing the maneuvers so that the cars can keep their lane. Using the MPC controller, Computer vision and Deep learning, more advance ADAS or Autonomous Vehicle can be designed for which will make our roads safer.

References

1. Ahmed, H.U., Huang, Y., Lu, P., Bridgelall, R.: Technology Developments and Impacts of Connected and Autonomous Vehicles: An Overview. **1**, 382–404, Smart Cities 5, USA (2022)

2. Yun, H., Park, D.: Virtualization of Self-Driving Algorithms by Interoperating Embedded Controllers on a Game Engine for a Digital Twining Autonomous Vehicle. **17**, 2102, Electronics 10, USA (2021)
3. Cui, H., et al.: Deep kinematic models for kinematically feasible vehicle trajectory predictions. In: 2020 IEEE International Conference on Robotics and Automation (ICRA), pp. 10563–10569. IEEE, Paris (2020)
4. Sazid, M.M., Haider, I., Rahman, M.E., Nuhel, A.K., Islam, S., Islam, M.R.: Developing a solar powered agricultural robot for autonomous thresher and crop cutting. In: 2022 12th International Conference on Electrical and Computer Engineering (ICECE), pp. 144–147, IEEE Dhaka, Bangladesh (2022)
5. Ganga, G., Dharmana, M.M.: MPC controller for trajectory tracking control of quadcopter. In: 2017 International Conference on Circuit Power and Computing Technologies (ICCPCT), pp. 1–6. IEEE, Kollam, India (2017)
6. Zohu, Z., Rother, C., Chen, J.: MPC Controller for trajectory tracking control of quadcopter. In: ICCPCT, pp.1–6, IEEE (2017)
7. Chen, S., Chen, H., Negrut, D.: Implementation of MPC-based path tracking for autonomous vehicles considering three vehicle dynamics models with different fidelities. Automotive Innovation **3**, 386–399 (2020)
8. Nuhel, A.K., Sazid, M.M., Bhuiyan, M.N.M., Arif, A.I., Roy, P.H., Islam, M.R.: Developing a Self-Driving Autonomous Car using Artificial Intelligence Algorithm. In: 2022 6th International Conference on Electronics, Communication and Aerospace Technology, pp. 1240–1249. IEEE, India (2022)
9. Alcalá, E., Puig, V., Quevedo, J.: LPV-MPC control for autonomous vehicles. IFAC-PapersOnLine **52**(28), 106–113 (2019)
10. Massaro, M., Limebeer, D.J.N.: Minimum-lap-time optimisation and simulation. Veh. Syst. Dyn. **59**(7), 1069–1113 (2021)
11. Nuhel, A.K., Sazid, M.M., Bhuiyan, M.N.M., Arif, A.I.: Designing and performance- analysis of a 3 DOF robotic manipulator arm and its higher order integration for 7 DOF robotic arm. In: 2022 4th International Conference on Sustainable Technologies for Industry 4.0 (STI), pp. 1–6, IEEE, Dhaka, Bangladesh (2022)
12. Mozaffari, S., Al-Jarrah, O.Y., Dianati, M., Jennings, P., Mouzakitis, A.: Deep learning-based vehicle behavior prediction for autonomous driving applications: a review. IEEE Trans. Intell. Transp. Syst. **23**(1), 33–47 (2020)
13. Peicheng, S., Li, L., Ni, X., Yang, A.: Intelligent vehicle path tracking control based on improved MPC and hybrid PID. IEEE Access **10**, 94133–94144 (2022)
14. Williams, T., et al.: Transportation planning implications of automated/connected vehicles on Texas highways. No. FHWA/TX-16/0–6848–1. Texas A&M Transportation Institute (2017)